Click Here for Full Article

Scaling tidal channel geometry with marsh island area: A tool for habitat restoration, linked to channel formation process

W. Gregory Hood[1]

[1] Hydraulic geometry and related analyses are often used to investigate tidal channel geometry and evolution and inform marsh restoration. An alternative approach is presented that avoids calculating tidal prism and allows analysis of additional channel metrics. It relies on scaling relationships between marsh island surface area and various metrics of the set of tidal channels draining each island. In the Skagit Delta marshes (Washington, United States), total channel surface area and length and surface area of the largest channel draining an island scaled disproportionately with island area, suggesting restoration of a 100-ha site would be preferable to restoration of 10 separate 10-ha sites to maximize channel length and area. A model of channel formation through random island conglomeration replicated observed scaling patterns, linking channel scaling to blind channel evolution from river distributaries. Channel size and complexity varied spatially, with significant deficits in an eroding marsh isolated from river distributaries and riverine sediments.

Citation: Hood, W. G. (2007), Scaling tidal channel geometry with marsh island area: A tool for habitat restoration, linked to channel formation process, *Water Resour. Res.*, *43*, W03409, doi:10.1029/2006WR005083.

1. Introduction

[2] Estuarine tidal channels are conduits for water, sediment, nutrients, detritus, and aquatic organisms and thus link the nearshore marine environment to highly productive tidal marshes [*Simenstad*, 1983; *Odum*, 1984; *Rozas et al.*, 1988; *Pethick*, 1992; *French and Spencer*, 1993]. Tidal channel geometry affects hydrodynamics [*Rinaldo et al.*, 1999], sediment transport [*French and Stoddart*, 1992], and the distribution and production of flora [*Sanderson et al.*, 2000] and fauna [*Levy and Northcote*, 1982; *Halpin*, 1997; *Williams and Zedler*, 1999; *Hood*, 2002a]. Consequently, understanding tidal channel geometry is key to understanding geophysical and ecological processes in tidal marshes and associated tidal flats.

[3] Tidal channel geometry has been investigated to develop metrics and analytic methods that contribute to understanding landform evolution [*Fagherazzi et al.*, 1999; *Rinaldo et al.*, 1999; *Marani et al.*, 2003; *Novakowski et al.*, 2004]; compare presumed anthropogenically degraded sites, restoration sites, and natural reference sites [*Hood*, 2002b]; provide pragmatic tools for design, prediction, and evaluation of habitat restoration actions [*Coats et al.*, 1995; *Zeff*, 1999; *Williams et al.*, 2002]; and predict the consequences of shoreline construction activities [*Renger and Partenscky*, 1974; *Hume*, 1991]. Just as terrestrial channels are sculpted by stream discharge, tidal channels are similarly sculpted by tidal prism. Thus geometric analysis has generally focused on cross-sectional channel geometry as predicted by tidal prism or contributing drainage area (hydraulic geometry)

[e.g., *Myrick and Leopold*, 1963; *Coats et al.*, 1995], or on the scaling of planform channel metrics with drainage area [e.g., *Rinaldo et al.*, 1999; *Marani et al.*, 2003; *Novakowski et al.*, 2004].

[4] Tidal prism is usually defined as the volume of water upstream of a channel cross section between mean lower low water (MLLW) and mean higher high water (MHHW). In addition to the upstream channel volume, tidal prism also includes the tidal volume of the contributing marsh plain. When marsh plains are not flooded by high tides, drainage boundary estimation is not necessary to calculate tidal prism. When they are partially flooded by high tides, marsh drainage boundaries can be measured through aerial photography of the flooded marsh [*Boon*, 1975] or detailed topographic surveys [*Renger and Partenscky*, 1974]. For extensively flooded marsh plains, hydrodynamic models have shown that drainage boundaries can be approximated by lines equidistant from channel axes [*Rinaldo et al.*, 1999; *Marani et al.*, 2003]. However, channels are not the only route for tidal exchange. Sheet flow across marsh boundaries directly into the ocean or river distributaries can account for significant tidal exchange over extensively flooded marshes [*Miller and Gardner*, 1981; *French and Stoddart*, 1992; *Davidson-Arnott et al.*, 2002; *Temmerman et al.*, 2005], which makes measurement of the marsh plain volume contributing to tidal channel flow problematic. Furthermore, vegetation density, height, and flexibility strongly affect sheet flow velocity [*Leonard and Luther*, 1995]. Because some plant species more effectively impede water flow than others, patchy vegetation can modify tidal energy distribution across the marsh surface, and this likely affects the real locations of marsh drainage boundaries independently of topography (because many marsh plant species have overlapping elevation distributions). In sum,

---

[1]Skagit River System Cooperative, LaConner, Washington, USA.

measurement of tidal prism can be time-consuming and labor-intensive, while estimation of contributing marsh area can be fraught with either real complications or simplifying assumptions.

[5] This paper illustrates an alternative, but related, approach to geometric analysis of tidal channels which requires little fieldwork, can be economically applied to a large population of tidal channels, and examines a different, potentially broader, set of channel metrics than does more traditional analysis. It is applicable even in areas where there is extensive marsh plain flooding and significant sheet flow, because it relies on neither the estimation of tidal prism nor contributing drainage area. Instead, it relies on the fractal nature of landforms [*Ouchi and Matsushita*, 1992; *Rodriguez-Iturbe and Rinaldo*, 1997] to develop allometric relationships [*Woldenberg*, 1966; *Church and Mark*, 1980; *Hood*, 2002a, 2002b] between the surface area of tidal marsh islands and various metrics of the set of tidal channels draining each island. Marsh islands have been chosen as a unit of geomorphological analysis because they are easily and unambiguously delineated and are relatively independent landscape units.

2. Setting

[6] The study area is located in the tidal marshes of the 308 km^2 Skagit River delta. The Skagit is the largest river flowing into Puget Sound (Washington, United States), providing about 34% of the freshwater input to the Sound. The river drains 8544 km^2 of the Cascade Mountains while cutting through valley terraces of Pleistocene glacial and dacitic Holocene lahar sediments [*Dragovich et al.*, 2000; *Beechie et al.*, 2001]. Elevations in the basin range from sea level to 3285 m. Mean annual precipitation ranges from 80 cm in the lowlands to over 460 cm in the mountains.

[7] More than 90% of the delta has been isolated from riverine and tidal influence by dikes and converted to agriculture and other uses [*Collins and Montgomery*, 2001]. Most of the remaining undiked wetlands are located at the outlets of the North and South Forks of the Skagit River (48°22′N, 122°29′W and 48°19′N, 122°22′W, respectively), which are the two principal river distributaries. Marsh sediments consist of organic-rich silt, silty clay and fine sand, while unvegetated tidal flats are fine to medium sand. Because of high river discharge, the marsh is oligohaline and vegetation (from low to high elevation) is dominated by *Scirpus americanus* (American threesquare), *Carex lyngbyei* (sedge), *S. validus* (soft stem bulrush), *Typha angustifolia* (cattail), *Myrica gale* (sweetgale), *Salix* spp. (willow), and *Picea sitchensis* (Sitka spruce). Semidiurnal tides range nearly 4 m and during higher high spring tides the marsh surface is inundated by up to 1.5 m of water. The upper limit of tidal influence is at river kilometer 13.

[8] Tidal channels in the Skagit marshes provide important rearing habitat for juvenile Chinook salmon (*Oncorhynchus tshawytscha*), which are listed under the Endangered Species Act as a threatened species in Puget Sound [*Fish and Wildlife Service*, 1999]. This habitat is also important to a wide variety of other fish and wildlife, ranging from commercially important invertebrates to marine mammals [*Simenstad*, 1983]. The threatened status of Chinook salmon has generated considerable interest in restoring tidal marsh and channel habitat in the Puget Sound

region. Planning for estuarine habitat restoration requires predictive tools to estimate how many and what size tidal channels can be generated and sustained by natural geophysical processes in a given area of restored marsh. This paper contributes to the development of such tools and to improved understanding of tidal marsh geomorphology.

3. Methods

[9] This study was limited to tidal marshes characterized by emergent and shrub vegetation [*Cowardin et al.*, 1979]. Unvegetated tidal flats and densely forested floodplains were not examined. Tidal channel margins and other shorelines visible in color infrared orthophotographs of the Skagit marshes were manually digitized in a GIS (Geographic Information System). The orthophotos were flown at an altitude of 1850 m on 30 August 2004 during a low tide of −0.3 m mean lower low water (MLLW) at a scale of 1:12,000 with 15-cm pixels. The smallest tidal channels that could be resolved in the photos were 30 cm wide. Channel margins and shorelines were defined by the abrupt transition from vegetated to unvegetated intertidal areas. Vegetated areas were typically characterized by reflectance signatures grading from white to red in the false-color infrared images (depending on plant species), while water was dark blue. Unvegetated sand flats ranged from bluish-gray to light gray, apparently depending on water content. Photosignatures were ground truthed to confirm photointerpretations, i.e., presence (and species) of vegetation, sand flats, and subtidal water observed in the field were correlated with photosignatures using obvious landmarks (channel junctions and meanders, vegetation patch patterns, large and stable logs) for orientation.

[10] Lidar (laser imaging, detection, and ranging) data for the study area were collected in April 2002 during a spring low tide from an altitude of 2300 m and had an average spacing of 3 m with a horizontal accuracy of 30 cm and vertical accuracy of 15 cm. The data were processed to produce a bare earth DEM (digital elevation model). Model error was determined by RTK GPS (real-time kinetic global positioning system) field survey (2 cm horizontal and vertical accuracy) of 696 points in the tidal marsh, where vegetation cover was simultaneously noted for each point. Differences between the lidar model and GPS measurements varied with vegetation cover (Table 1). In early April, most marsh vegetation is only a few centimeters high (*C. lyngbyei*, *Eleocharis palustris*, *S. americanus*) or sparsely present (*S. validus*, *T. latifolia*), so that the ground is essentially bare and lidar GPS differences are negligible. At slightly higher elevations, *T. angustifolia* is common, 1.5 to 2 m tall, and grows more densely so that lidar overestimates ground elevation by an average of 0.24 m due to vegetation cover. At still higher elevation, dense 2-m-high shrub thickets are common and lidar overestimates ground elevation by an average of 0.69 m with considerably more variable error than for the other vegetation, probably due to greater variation in canopy height and density. Because plant canopy height and density are correlated with ground elevation, so are lidar overestimates of ground elevation, i.e., lidar errors are biased. GIS analysis generated mean elevations for each marsh island (exclusive of the tidal channels) to be used as a covariate in statistical analysis. Biased error exaggerates the effect of the covariate and

Table 1. Mean Discrepancy Between Lidar and Survey-Grade GPS Measurements of Marsh Elevation, Depending on Vegetation Cover[a]

Parameter	Bare Ground	Low Emergent Vegetation	*T. angustifolia*	Shrubs
Mean GPS elevation	0.42	1.04	1.13	1.32
Mean lidar − GPS	−0.02	0.05	0.24	0.69
Variance of lidar − GPS	0.12	0.15	0.15	0.58
Count of lidar − GPS	11	400	193	92

[a]Low emergent vegetation includes *C. lyngbyei, E. palustris, S. americanus, S. validus,* and *T. latifolia.* Shrub vegetation is primarily *M. gale* but includes *Salix* spp., *Lonicera involucrata,* and *Rosa nutkana.* Elevation is relative to NGVD 1929, in meters. Mean sea level is 0.18 m, MLLW is −1.89 m, and MHHW is 1.68 m.

increases the probability of a type I statistical error, while decreasing the probability of a type II error. As will be seen later, this had no effect on interpretation of the results because the null hypothesis with respect to the covariate was not rejected.

[11] Tidal channel geometry was examined from an allometric perspective [*Woldenberg*, 1966; *Bull*, 1975; *Church and Mark*, 1980]. A system is allometric when the relative rate of change of one part of a system (y) is proportional to the relative rate of change of another part of the system (x), or of the whole system. Allometric models are related to fractal ones and both are described by power functions, $y = ax^b$, which can be linearized through log transformation. Landforms are self-affine fractals, i.e., form is ''stretched'' depending on scale [*Ouchi and Matsushita*, 1992; *Rodriguez-Iturbe and Rinaldo*, 1997], which is fractal terminology for allometry [*Mandelbrot*, 1983]. Allometry and fractal geometry differ in perspective: fractal geometry generally focuses on how a measured quantity varies as a power of measurement scale [*Milne*, 1991], whereas allometry focuses on proportional relative rates of change between two measured quantities in a system. In this study, linear regression of log-transformed data was used to evaluate allometric relationships between marsh island area and various channel metrics. Mean island elevation was included as an additional independent variable to control for
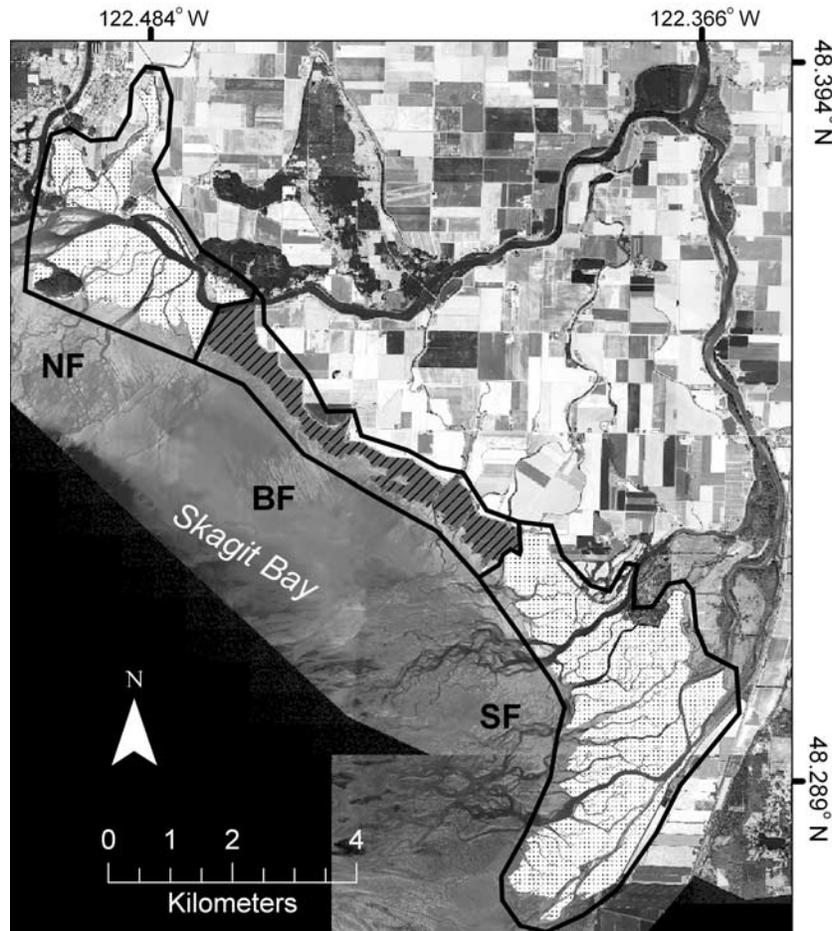

Figure 1. Location of the North Fork (NF), South Fork (SF), and bay fringe (BF) marshes in the Skagit River Delta. Areas landward of the marshes are generally farmland protected from tidal and riverine flooding by dikes and levees. River distributaries from the North Fork Skagit River that once emptied into the bay fringe marsh were diked at their inlets and near their outlets in the 1950s so that distributary flow to this area no longer occurs. The South Fork marshes are dissected by numerous river distributaries that broadly disperse riverine flow, while the smaller North Fork marshes have fewer river distributaries with a single channel dominating riverine discharge.

Figure 2. Remnant pedestals of eroded tidal marsh, common in the bay fringe area of the Skagit Delta. These marsh pedestals are not present in the North or South Fork marshes, where rapid progradation has been occurring over the last century.

the possible influence of elevation on channel geometry [e.g., *Allen*, 2000; *Temmerman et al.*, 2005].

[12] Area and perimeter of tidal marsh islands and blind tidal channels (tidal channels with a downstream, but no upstream, connection to another water body) were calculated with a GIS. Island area did not include the area of the blind tidal channels draining the islands to avoid spurious correlation between island area and channel metrics, particularly those involving channel area. Channel length was calculated as half of the channel perimeter and included the lengths of the channel main stem and all of its tributaries. Channel count was defined as the number of channel outlets on an island's perimeter. Magnitude was the count of first-order channels in a channel network, and provided an indication of network complexity. Channel surface area, length, and magnitude were summed over all channels draining an island to provide a collective total for each island. They were also calculated and analyzed for the largest channel draining each island. Additionally, the main stem length of each island's largest channel was calculated to facilitate comparison of results with other studies, and the number of tributary channels to the main stem of each island's largest channel were counted as another indication of network complexity.

[13] Marsh-channel scaling patterns were compared among five groups of marsh islands: North Fork true islands, North Fork dike-adjacent islands, South Fork true islands, South Fork dike-adjacent islands, and bay fringe marsh (where all but one island were dike adjacent). Dikes bounded 20–40% of the perimeter of dike-adjacent islands, with the remainder bounded by river distributaries or Skagit Bay. North Fork islands were located at the mouth of the North Fork distributary of the Skagit River, while South Fork islands were at the South Fork outlet (Figure 1). The bay fringe marsh, between the North and South Fork marshes, has been isolated from riverine sediment inputs since river distributaries to this area were diked off in the

1950s. Consequently the bay fringe marsh has experienced significant surface erosion resulting in 40-cm-high pedestals of thickly vegetated remnant marsh surrounded by sparsely vegetated lower-elevation marsh (Figure 2). In contrast, the North and South Fork marshes have experienced significant progradation since at least 1889 [*Hood*, 2006]. Thus the spatial extent of the bay fringe marsh was defined by isolation from distributary channels and the presence of marsh pedestals indicating erosion. Casual visual inspection suggests tidal channels in the bay fringe area are less numerous or complex than in the North or South Fork marshes. Allometric comparison was used to objectively evaluate this potential difference. Finally, marsh islands without tidal channels were not examined, except to note that they were generally smaller than the smallest islands with tidal channels.

3.1. Geometric Model

[14] A simple geometric model was developed to link observed patterns in tidal channel metrics to the geomorphic process of tidal channel development. Blind tidal channels in the Skagit marshes originated from the coalescence of marsh islands during delta progradation with concomitant narrowing of intervening distributary channels. The narrowed distributaries were obstructed by sediment, usually near their landward end, leaving blind tidal channels which are now dependent on tidal flushing of sediments to persist. This process has been shown to generate tidal channels as narrow as 30 cm [*Hood*, 2006].

[15] This channel formation process was mimicked by a simple geometric model of marsh island conglomeration and channel pattern generation, the random island conglomeration model (RIC), with the following simplifying assumptions and rules: (1) Marsh islands were represented by an integer multiple of unit squares. (2) Island coalescence was represented by the junction of two unit squares to form an island conglomeration, recurrent junction of island
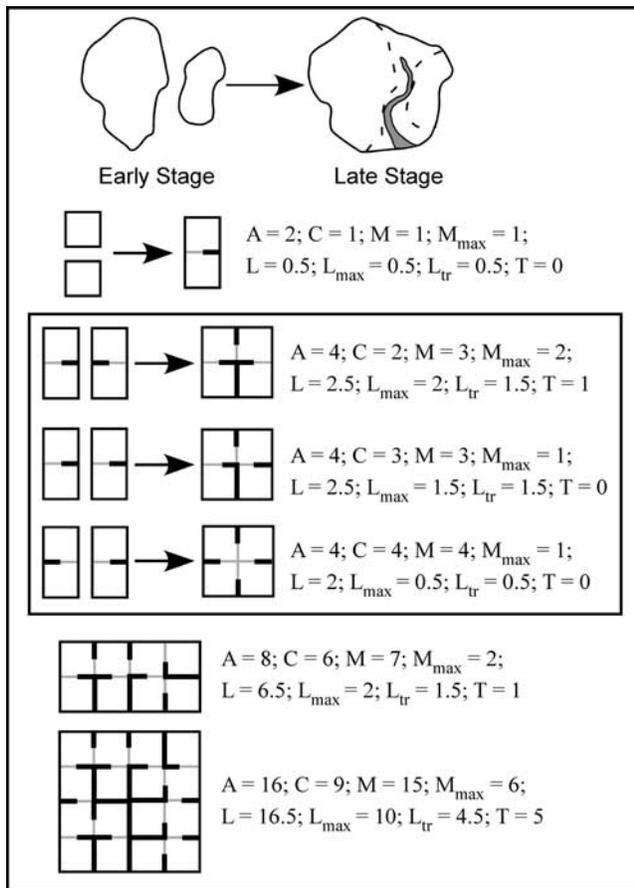
Figure 3. Illustration of the geometric model of tidal channel network development in the Skagit Delta. Formation of all possible two-square and four-square islands is shown, along with random examples of larger islands. Thick lines represent island perimeters and tidal channels. Light lines represent unit squares of conglomerated marsh. Channel metrics are displayed to the right of each illustration: A, island area; C, count of channels in an island; M, island magnitude; M_{max}, magnitude of the largest channel; L, total channel length; L_{max}, length of the longest channel; L_{tr}, length of the main stem or trunk of the longest channel; T, count of the tributaries to the main stem.

conglomerates formed increasingly larger square or rectangular conglomerations; irregularly shaped islands were not considered. (3) Tidal channels were represented by some fraction of the junction between two unit squares or two island conglomerations. In the case where two unit squares were joined, one channel resulted which was half the length of the juncture, i.e., had length of 1/2. In the case where two island conglomerations were joined, two channels resulted, one which had length of 1/2 at one end of the junction and one whose length was variable and extended from the other end of the junction to the most upstream tributary to the junction. This unequal channel formation represented an upstream/downstream polarity to the junction typical of observed channel formation. A limitation of this model was that it could not generate metrics related to channel width or surface area. Thus comparisons between this model and the observed marshes were limited to metrics related to channel length and network complexity.

[16] Island conglomerations were formed by randomly orienting and joining smaller island conglomerations recursively to create larger islands. Modeled islands ranged in size from 2 to 512 unit squares, a scale comparable to that observed in the Skagit marshes. The RIC model included the single possible 2-unit island, all three possible 4-unit configurations (Figure 3), and 10 random samples each of 6-, 8-, 12-, 16-, 20-, 24-, 32-, 40-, 48-, 64-, 88-, 128-, 176-, 256-, 352-, and 512-unit islands for a total sample size of 164 island conglomerations.

3.2. Statistical Analysis

[17] Island area and dependent variables describing various aspects of channel geometry were log transformed for linear regression analysis to equalize variance in the residuals and to fit power functions. The slope of the fitted regression lines is equal to the exponent of the power functions, i.e., the scaling exponent. Regression lines were compared among the five marsh island groups by analysis of covariance (ANCOVA) using model I regression [*Zar*, 1984]. Model I regression assumes independent variables are not subject to random error or are controlled by the experimenter. In this study the independent variable was not a random sample from a population. Instead, the entire population of channelized marsh islands was observed for each of the five island groups. Additional reasons for using model I regression were (1) measurement error for island area was low compared to dependent channel metrics, i.e., island boundaries were easy to distinguish while small channels were relatively more difficult to distinguish depending on vegetation cover, sun angle (shadow and glare), and photo resolution and (2) there was a theoretical basis for a causal link between independent and dependent variables, i.e., marsh area affects the amount of tidal prism available to maintain channel form [*Sokal and Rohlf*, 1995]. Initially, the mean topographic elevation of each island was an additional covariate. However, it had no statistical significance as a predictor of channel geometry and was therefore dropped from the analysis.

[18] When regression slopes were not significantly different between marsh island groups, a common regression slope was calculated for the five groups from the ANCOVA [*Zar*, 1984]. Following ANCOVA, the Student-Newman-Keuls (SNK) test was employed for post hoc comparisons of regression elevations (i.e., vertical position on a graph) between groups [*Zar*, 1984]. The criterion for statistical significance was $p < 0.05$. Regression slopes derived from the RIC model were compared to the 95% confidence intervals of the common regression slopes for the Skagit marsh data. Model-derived slopes within the 95% confidence interval were considered comparable to ANCOVA-derived common regression slopes.

[19] The minimum island area capable of supporting tidal channel development was calculated from the regression data using inverse prediction, i.e., estimation of the expected value of an independent variable from a specified value of the dependent variable [*Zar*, 1984]. The common slope and the common regression residual mean sum of squares from a three-group ANCOVA (North Fork, South Fork, and bay fringe marshes) were used for inverse prediction. The three-group ANCOVA did not distinguish between dike adjacent marsh and true islands because the previously described five-group ANCOVA found no differ-

Table 2. Analysis of Covariance Summaries

Channel Metric	Test for Regression Slope Heterogeneity		Test for Regression Elevation Heterogeneity		Multiple R^2
	$F_{4,67}$	p	$F_{4,71}$	p	
Count	0.608	NS	5.505	< 0.001	0.79
Island magnitude	1.070	NS	6.670	< 0.001	0.86
Magnitude of largest channel	0.261	NS	5.406	< 0.001	0.78
Total channel length	0.446	NS	8.170	< 0.001	0.92
Length of largest channel	0.203	NS	6.441	< 0.001	0.86
Trunk length	0.719	NS	3.991	< 0.01	0.84
Tributaries + 1	0.259	NS	4.328	< 0.005	0.76
Total channel surface area	1.654	NS	12.425	< 0.001	0.92
Surface area of largest channel	0.589	NS	8.619	< 0.001	0.87
Outlet width of largest channel	0.254	NS	4.570	< 0.002	0.74

ences. Minimum island area was calculated from data on channel count and island magnitude because these channel metrics had an unambiguous threshold (0 versus 1), while defining a practical a priori length, width, or area threshold was problematic: Field observations suggest channels cease to exist long before lengths, widths, or areas of zero are reached.

4. Results

[20] Mean and median island elevation, and the proportion (arcsin-square-root transformed) of an island below mean high water (or any of several other arbitrary elevations) were highly correlated with each other (r > 0.995). Thus mean elevation was considered a sufficient index of island elevation. Marsh island area and mean elevation were uncorrelated (r = 0.22), as required for multiple regression. However, mean island elevation was not a significant predictor for any channel metric, despite its exaggerated effect due to biased lidar error. Because theory suggests elevation effects on channel geometry are greatest at intermediate elevations [*Allen*, 2000], and because regression and ANCOVA assume linear relationships, subsets of the data were examined for curvilinear relationships between island elevation and channel metrics. Three subsets of approximately similar-sized islands (2.0 to 3.6 ha, 13.2 to 18.8 ha, and 38.5 to 50.6 ha; with n = 16, 11, and 10, respectively; and with mean elevations ranging from −1.3

to 0.6 m, −0.7 to 0.5 m, and −0.8 to 0.6 m MLLW, respectively) were selected to keep the effects of island area relatively constant. Island size ranges for the data subsets represented 2 to 14% of the range of the entire data set, while subset elevation ranges spanned 57 to 90% of the range of the entire data set. None of the data subsets showed any relationship between elevation and any of the channel metrics. Consequently, island elevation was omitted from further analysis.

[21] All observed aspects of tidal channel geometry scaled with island area, with r^2 ranging from 0.74 for channel outlet width to 0.92 for total channel length and total channel surface area. ANCOVA indicated that for each channel metric, regression slopes were homogeneous among all groups examined, while regression elevations were heterogeneous (Table 2). The common scaling exponent was 1.56 for total channel surface area, 1.26 for total channel length, and 1.41 for the channel surface area of the largest channel of an island (Table 3). Scaling exponents greater than 1 indicate these channel metrics increased more rapidly than island area. Channel metrics whose scaling exponents did not differ significantly from 1 increased proportionately to island area. These included island magnitude, and magnitude and length of the largest channel in an island. The remaining channel metrics increased more slowly than island area. None declined with increasing island area.

Table 3. Regression Elevations (Back Transformed for Use as a Power Function Coefficient) and Slopes (Scaling Exponents) for a Variety of Channel Metrics Versus Island Area[a]

Channel Metric	Observed Regression Elevation			Observed Slope and 95% Confidence Interval	Model Slope and 95% Confidence Interval
	NF	SF	BF		
Count	1.04	1.81	1.04	0.53 − **0.63** − 0.73	0.61 − **0.63** − 0.65
Island Magnitude	1.34	2.22	0.59	0.89 − **1.04** − 1.20	1.02 − **1.03** − 1.04
Magnitude of largest channel	1.31	1.31	0.34	0.67 − **0.85** − 1.04	0.99 − **1.02** − 1.06
Total channel length	70.4	70.4	19.6	1.12 − **1.26** − 1.39	1.14 − **1.15** − 1.16
Length of largest channel	54.0	54.0	14.4	0.90 − **1.06** − 1.22	1.03 − **1.07** − 1.10
Trunk length	50.6	50.6	22.4	0.66 − **0.76** − 0.86	0.60 − **0.63** − 0.65
Tributaries + 1	1.33	1.33	0.51	0.54 − **0.65** − 0.77	0.68 − **0.71** − 0.74
Total channel surface area	0.0024[b]	0.0052	0.0008	1.38 − **1.56** − 1.75	
Surface area of largest channel	0.0026	0.0041	0.0006	1.15 − **1.41** − 1.67	
Outlet width of largest channel	0.80	1.30	0.80	0.52 − **0.66** − 0.81	

[a] All values for the Skagit data are ANCOVA derived. A common estimate was derived for groups whose elevations were not significantly different. Regression slopes (bold) are flanked by upper and lower limits of their 95% confidence intervals. NF, North Fork marshes; SF, South Fork marshes; BF, bay fringe marshes.
[b] Only includes the true islands because their elevation differed significantly from the dike-adjacent marsh.
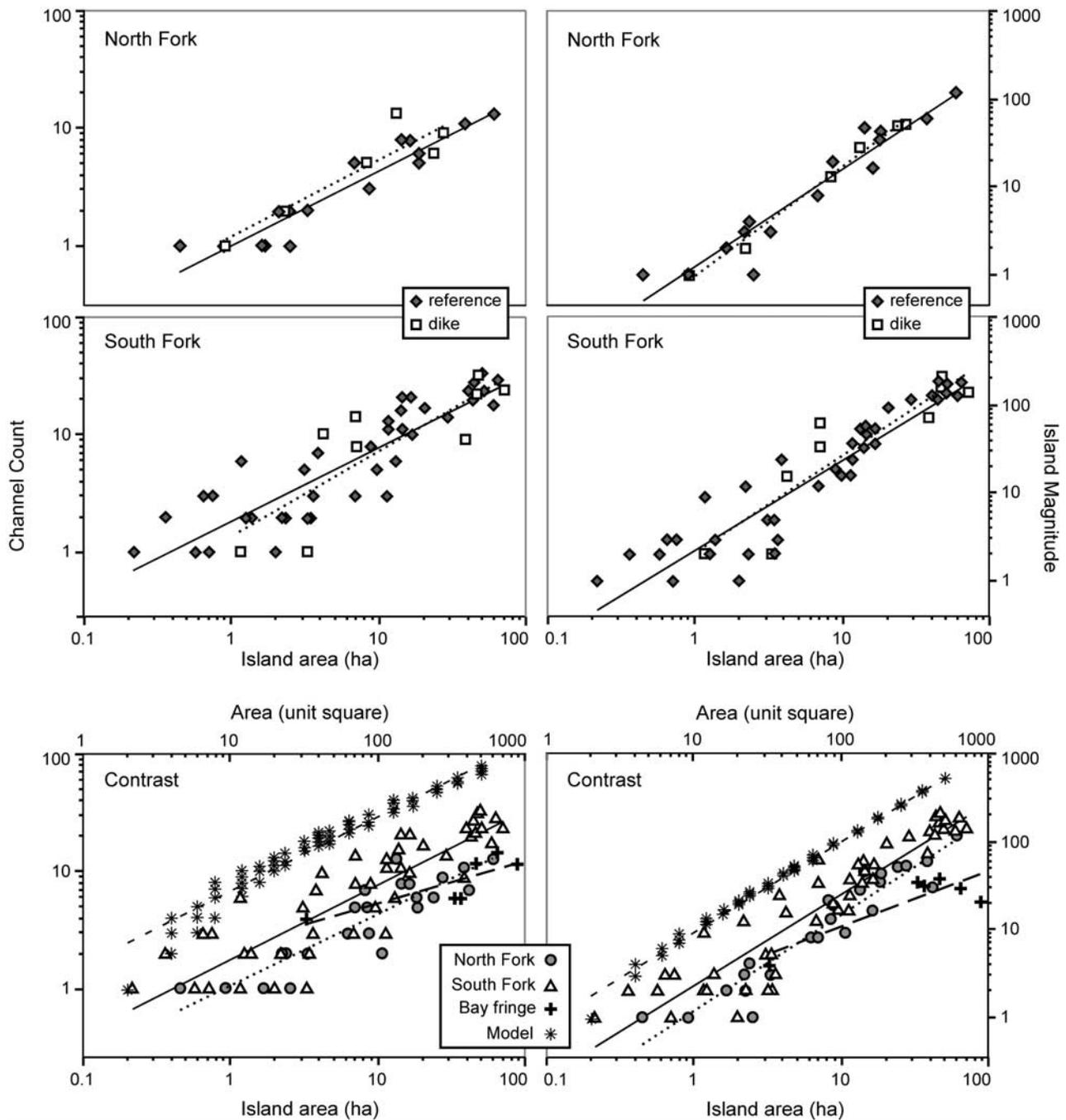
Figure 4. (left) Channel count and (right) island magnitude scaling with marsh island size for the (top) North and (middle) South Fork marshes, where true islands are compared to dike-adjacent marshes. (bottom) Because there were no statistically significant differences between them, dike adjacent marshes and true islands are grouped together to facilitate graphic comparison between North Fork, South Fork, and bay fringe marshes as well as comparison to the results of the RIC model (upper abscissa). See Table 3 for regression parameter estimates for Figure 4 (bottom).

[22] Post hoc comparisons indicated regression elevations did not differ between reference and dike-adjacent islands for North or South Fork marshes, with one exception. Total channel surface area was greater for dike-adjacent compared to reference islands in the North Fork marshes ($p < 0.05$), probably because large ditches have been excavated and widened in several dike-adjacent islands in the North Fork marshes to facilitate drainage of nearby agricultural lands.

This increased channel surface area in these areas without affecting other channel metrics.

[23] Post hoc comparisons showed significant differences in regression elevations between the bay fringe marshes and all other groups for all channel metrics except channel count, outlet width of the largest channel of an island, and island magnitude (Figures 4–8). In the case of channel count and outlet width there were no differences between
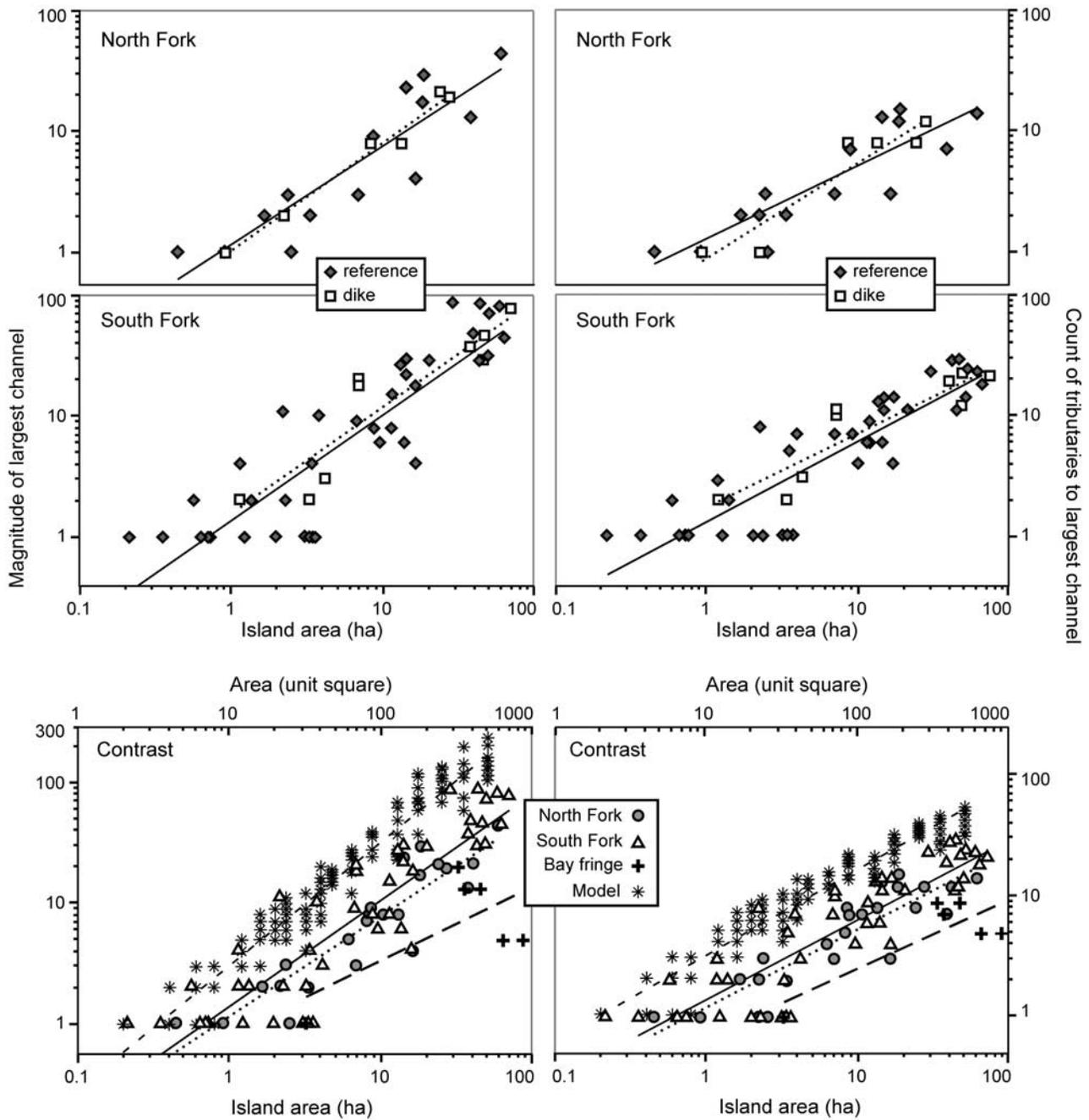
Figure 5. (left) Scaling of the magnitude and (right) tributary count for the largest channel in a marsh island with marsh island size for the (top) North and (middle) South Fork marshes, where true islands are compared to dike-adjacent marshes. (bottom) Because there were no statistically significant differences between them, dike adjacent marshes and true islands are grouped together to facilitate graphic comparison between North Fork, South Fork, and bay fringe marshes as well as comparison to the results of the RIC model (upper abscissa). See Table 3 for regression parameter estimates for Figure 5 (bottom).
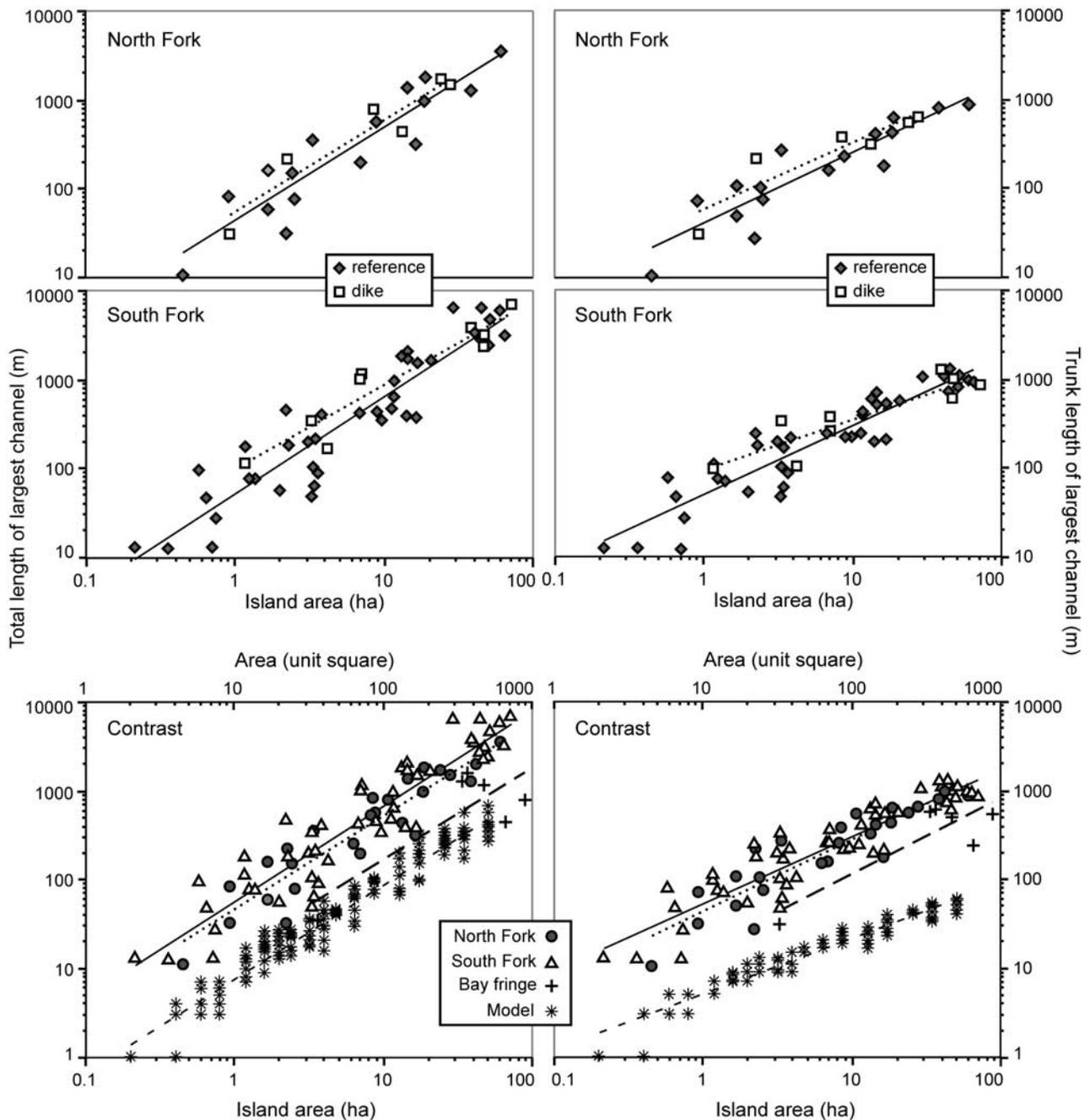
Figure 6. (left) Scaling of the total and (right) trunk length of the largest channel in a marsh island with marsh island size for the (top) North and (middle) South Fork marshes, where true islands are compared to dike-adjacent marshes. (bottom) Because there were no statistically significant differences between them, dike adjacent marshes and true islands are grouped together to facilitate graphic comparison between North Fork, South Fork, and bay fringe marshes as well as comparison to the results of the RIC model (upper abscissa). See Table 3 for regression parameter estimates for Figure 6 (bottom).
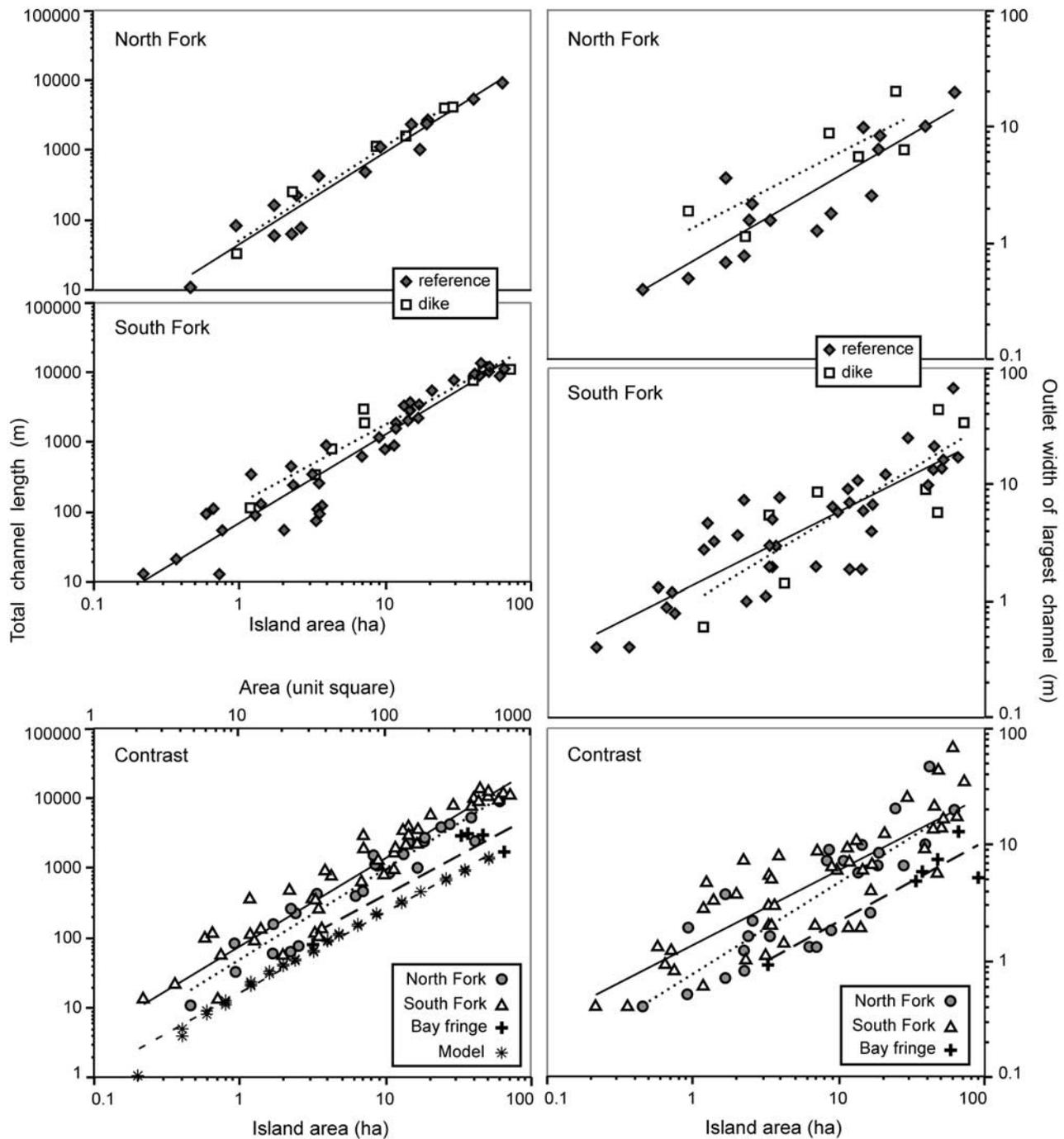
Figure 7. (left) Total channel length and (right) outlet width scaling with marsh island size for the (top) North and (middle) South Fork marshes, where true islands are compared to dike-adjacent marshes. (bottom) Because there were no statistically significant differences between them, dike-adjacent marshes and true islands are grouped together to facilitate graphic comparison between North Fork, South Fork, and bay fringe marshes as well as comparison to the results of the RIC model (upper abscissa, bottom left). See Table 3 for regression parameter estimates for Figure 7 (bottom).

the bay fringe marshes and either the North Fork reference or dike-adjacent islands, while for island magnitude there was no difference between the bay fringe marshes and North Fork dike-adjacent islands. South Fork reference and dike-adjacent islands differed from bay fringe marshes for all channel metrics. In general, the bay fringe marshes had smaller and less complex tidal channels than the North

or South Fork marshes, and fewer channels than the South Fork marshes. Total channel length, and length and magnitude of the largest channel draining an island were more than three times greater for the North and South Fork marshes than for the bay fringe marshes, while trunk length and tributary count were more than two times greater (Table 3, compare regression elevations). Total channel
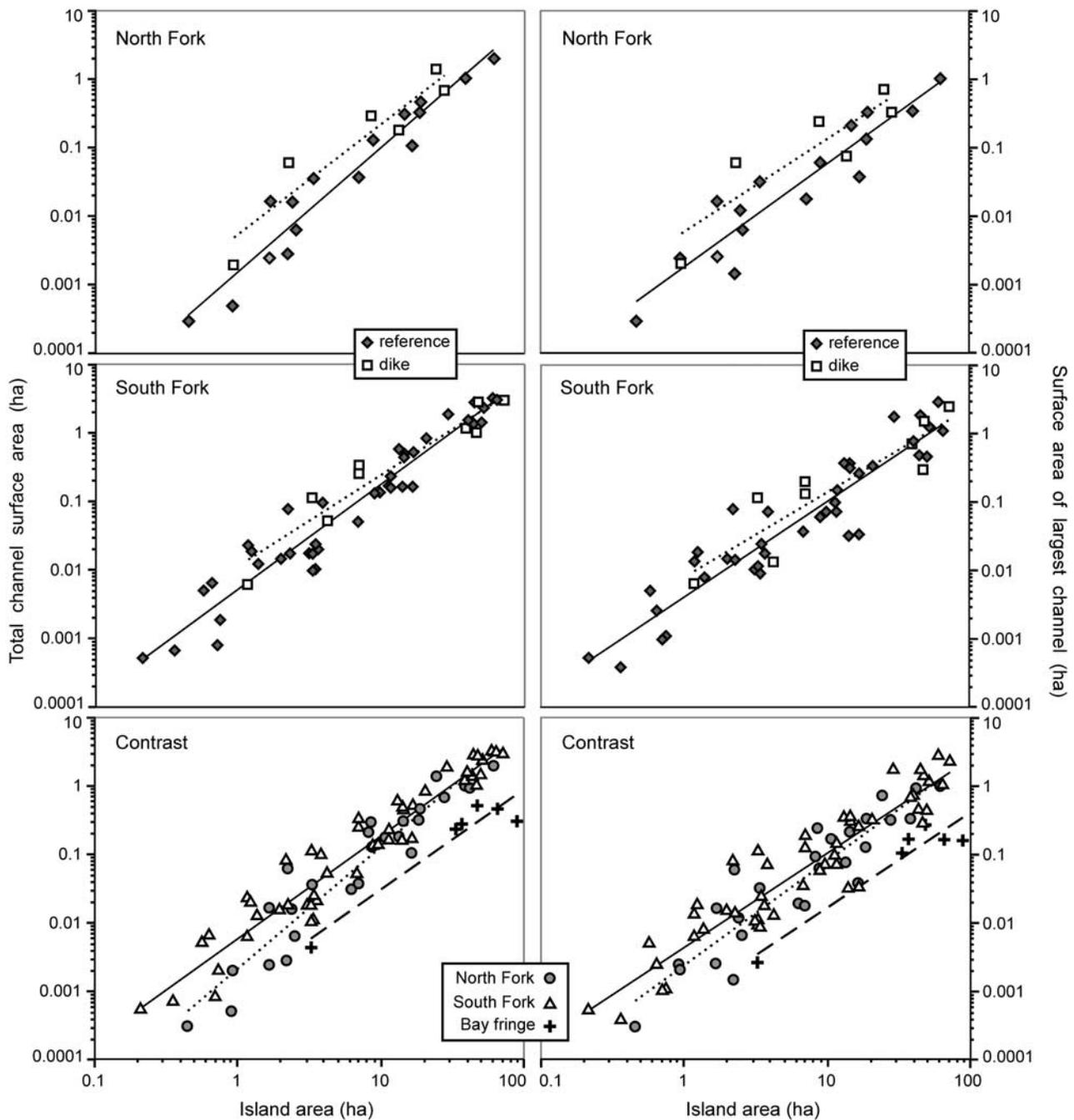
Figure 8. (left) Scaling of total channel surface area and (right) the surface area of the largest channel in a marsh island with marsh island size for the (top) North and (middle) South Fork marshes, where true islands are compared to dike-adjacent marshes. (bottom) Dike-adjacent marshes and true islands are grouped together to facilitate graphic comparison between North Fork, South Fork, and bay fringe marshes. See Table 3 for regression parameter estimates for Figure 8 (bottom).

surface area and the surface area of the largest channel were more than six times greater in the South Fork marshes than the bay fringe marshes, and threefold and fourfold greater, respectively, for the North Fork versus bay fringe marshes.

[24] Regression elevations differed between the North and South Fork reference islands for half of the observed channel metrics. Compared to the North Fork, South Fork islands had more than 1.6 times the channel count, island

magnitude, total channel surface area, and surface area and outlet width of the largest channel in an island.

[25] Inverse prediction indicates that the minimum island area capable of sustaining a tidal channel ranges from 0.75 to 0.94 ha for the North Fork marshes, 0.39 to 0.46 ha for the South Fork marshes, and 0.94 to 1.66 ha for the bay fringe marshes (Table 4). The 95% confidence limits are fairly large because the island area estimates are for the

Table 4. Inverse Prediction of the Minimum Island Area That Sustains a Tidal Channel, Depending on Marsh Site and Channel Metric Examined[a]

Metric	North Fork Marsh	South Fork Marsh	Bay Fringe Marsh
Channel count	0.12 − **0.94** − 4.92 (4.06)	0.07 − **0.39** − 2.01 (1.68)	0.00 − **0.94** − 13.78 (4.06)
Island magnitude	0.17 − **0.75** − 2.79 (1.33)	0.12 − **0.46** − 1.62 (0.82)	0.00 − **1.66** − 11.52 (2.94)
Observed minimum island area, ha	0.45	0.21	not applicable

[a] Minimum island areas (bold) are flanked by upper and lower limits of their 95&percnt; confidence intervals. The minimum island area which would produce equivalent regression elevations for the RIC model are shown in parentheses. The model unit square equals one half the minimum island area. Observed minimum island area is the minimum data value associated with channel count and island magnitude of 1. Note that inverse prediction produces asymmetrical confidence intervals, which is further accentuated here by back transformation of logarithmic data.

lower limit of the data range and regression confidence bands flare out toward the ends of the data range. Additionally, a large range of island sizes have channel counts and island magnitudes of 1. The smallest islands in this range and their channels may not be in relative equilibrium, i.e., these channels may be relatively ephemeral. For example, the 0.21-ha South Fork island developed a small channel along its margin as a consequence of island progradation between 1998 and 2000, according to high-resolution orthophotos [*Hood*, 2006]. It is possible this very new channel will not persist. The only other South Fork island with channel count and magnitude of 1 amounted to 1.99 ha. The channel in the smallest North Fork island was similarly formed along a prograding island margin, although between 1980 and 1991, and it appears to be filling in: It has soft unconsolidated sediments compared to the firm sandy bottoms of typical channels. The channel in the next smallest North Fork island is entirely filled with LWD and thus also appears to be filling in. This leaves a 0.93-ha island as the smallest North Fork island sustaining a single unbranched channel.

[26] Channel metrics derived from the RIC model scaled with island size similarly to the empirical Skagit marsh observations (Table 3 and Figures 4–7). Scaling exponent estimates for model and marsh data were identical, or nearly so, for channel count, island magnitude, and length of the largest channel in an island. Model estimates were within the 95% confidence limits of marsh exponent estimates for the magnitude and tributary count of the largest channel in an island and for total channel length. Only trunk length scaling differed between the model and marsh observations, but adjoining 95% confidence limits indicated these differences were slight.

[27] The unit squares of the RIC model require assignment of some quantity of area before model regression elevations have any meaning. A further test of the model occurs by determining what assigned areas produce model regression elevations matching those observed for the Skagit marshes, and comparing those areas to the inverse regression estimates of minimum channelized island area. Note that two unit squares are required to form the minimum channelized island. The results of such a comparison (Table 4) show that the model minimum channelized island areas required to match marsh regression elevations fit within the 95% confidence intervals of the inverse predictions. This test of the RIC model is weaker than the comparison of regression slopes (scaling exponents) because the confidence intervals for the regression elevations are wider than those for the regression slopes. Nevertheless, this comparison does further illustrate general consistency between the model and empirical observations.

5. Discussion

[28] The goal of the RIC model was to show that observed tidal channel network scaling in the Skagit marshes could be linked to blind channel network formation through recursive marsh island conglomeration, a process that has been previously documented for the Skagit marshes [*Hood*, 2006]. While it is conceivable that the same set of scaling patterns could be reproduced through a variety of arbitrary models, the relevant comparison is not between unrelated models, but between observed scaling patterns and a model that mimics an observed process. Although the RIC model is simplistic, it nevertheless replicated scaling patterns observed in the Skagit marshes for 6 of 7 channel metrics, with the seventh metric differing little between the model and the marshes. Similarly, the model provided estimates of minimum channelized island area that were generally consistent with empirical observations (when equivalent regression elevations were assumed for the model and empirical data), although this was a considerably weaker test of the model due to wide confidence intervals around the inverse predictions of minimum channelized island area. The RIC model illustrates the role of chance in tidal channel formation through island conglomeration, but not the role of necessity [*Rodriguez-Iturbe and Rinaldo*, 1997]. Thus the RIC model is an encouraging first step toward development of a more sophisticated modeling approach that would include necessity, i.e., sediment transport processes that affect channel form and persistence (e.g., channel filling and narrowing), and that would address metrics related to channel width or surface area.

[29] Tidal channel geometry in the Skagit marshes appears to be a function of both island conglomeration history, which affects the particular spatial organization of the tidal channels; and tidal prism, which affects channel size. For example, dike construction reduces the tidal prism of marshes remaining seaward of the dikes and this leads to channel shoaling and narrowing seaward of the dikes [*Hood*, 2004]. Nevertheless, dike adjacent marshes have similar channel scaling as true islands. Just as blind channels obstructed by dikes reach an equilibrium size depending on available tidal prism, so do distributary channels naturally converted to blind tidal channels by sediment and large woody debris (LWD) obstructions during island conglomeration. Thus shared island conglomeration history and tidal environments lead to similar scaling for dike-adjacent and true island marshes and their channels.
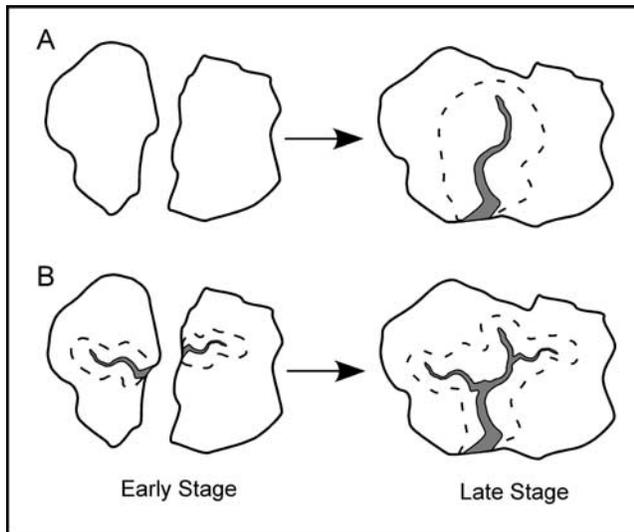
Figure 9. Tidal prism partitioning between channelized and sheet flow increases with marsh island conglomeration. Scenario A shows the simplest contrast between two islands without tidal channels where all tidal prism is sheet flow across the island margins and the conjoined islands where their junction forms a tidal channel whose drainage divide (dashed line) partitions island tidal prism into channel-directed flow within the divide and sheet flow across the island margin outside of the divide. Scenario B shows a similar contrast except the two early stage islands already have some tidal channel drainage. In both cases, the channelized portion of tidal prism increases to a greater degree than island area.

[30] Where marshes experience extensive tidal flooding, tidal prism is obviously proportional to island size, but the fraction of tidal prism moving through tidal channels versus across the marsh margin directly to or from a distributary or bay likely scales with island size. Consider a simple island conglomeration scenario (Figure 9) where two small islands without tidal channels coalesce to form a larger island with a new channel along the junction of the two small islands. The banks of the new channel were formerly island margins and water that once drained across those island margins now drains into the new channel. The two original islands had no channelized tidal prism, while the new conglomerated island does. Similar repartitioning of tidal flow occurs with the conglomeration of larger, channelized islands. Channel tidal prism increases with the additional volume of the new channel formed by the island junction, and with the development of a new drainage basin for that channel. The only study providing any data on this issue [*Williams et al.*, 2002] showed that channel tidal prism scaled with marsh area with an exponent of 1.17, i.e., channel tidal prism increased faster than marsh area. Thus, while several studies have shown that tidal flow across marsh margins, rather than through tidal channels, can amount to nearly 50% of total marsh tidal prism [*Miller and Gardner*, 1981; *French and Stoddart*, 1992; *Davidson-Arnott et al.*, 2002; *Temmerman et al.*, 2005], these results are likely scale-dependent with smaller marshes having a larger proportion of nonchannelized tidal prism (assuming comparable elevations and tide ranges amongst comparisons).

[31] Suspected differences in tidal channel abundance, size, and complexity between the North and South Fork marshes versus the bay fringe marshes were confirmed and quantified by allometric comparisons between the areas, reflected in large differences in regression elevations. These differences coincide with observations of significant marsh erosion in the bay fringe marshes compared to significant marsh progradation in the North and South Fork marshes over the last century [*Hood*, 2006]. Erosion of the bay fringe marshes is due to obstruction of large distributary channels to this area by dikes during the 1950s. Distributary obstruction ended riverine sediment export to the bay fringe and caused local sediment starvation. This illustrates a potential application of allometric landform analysis: diagnosis of anthropogenic alteration of geomorphic processes and elucidation of its consequences for landforms.

[32] Differences in tidal channel geometry between the North and South Fork marshes were not anticipated prior to this study, because they were not obvious from casual examination of air photos or during fieldwork for other studies. Nevertheless, allometric analysis indicated clear differences for half of the channel metrics examined, although they were considerably less than for comparisons between these areas and the bay fringe marsh. The observed differences in North and South Fork channel geometries might be explained by a variety of physical differences between the sites. For example, the South Fork carries 45% of the Skagit River flow versus 55% for the North Fork, but South Fork marsh area is three times that of the North Fork marsh. The South Fork also has considerably more channel distributaries than the North Fork. All of these factors combine to distribute river discharge over a larger area in the South Fork compared to the North Fork and weaken its influence relative to tidal forces. Additionally, the North Fork marshes are exposed to considerable fetch from southerly storm winds, while the South Fork marshes are sheltered in comparison. Finally, the North Fork marshes are on average 22 cm higher than the South Fork marshes. This list is not a satisfactory explanation for channel geometry differences between the North and South Forks, because the mechanisms by which these variables might influence channel geometry are poorly understood or quantified. The exception is marsh elevation. Tidal channel geometry is thought to have maximum expression at intermediate elevations [*Allen*, 2000; *Temmerman et al.*, 2005], but this study found no relationship between mean island elevation and channel geometry. One explanation may be that channel depth rather than planform geometry was responsive to variation in marsh elevation. Another explanation is that this study examined a relatively narrow range of elevations. Channels in low-elevation unvegetated sand flats were not examined, nor were those at high elevations which have mostly been converted to agriculture or have forest canopies that obscure the few remaining areas of marsh. Yet another possibility is that the scale of this study was too coarse to resolve elevational influences. Channels and elevations were only resolved to the island scale, but large channels pass through a range of elevations while draining an island. In contrast, *Temmerman et al.* [2005] described the influence of elevation on channel geometry at the reach scale. Likewise, *Feola et al.* [2005] found spatial heterogeneity in channel geometry on the scale of 10s to

100s of meters (subbasins within a marsh island) that they attributed to possible spatial variation in topography, soil type, vegetation cover and structure, and biostabilization and bioturbation, among other factors.

[33] Similar scaling for dike-adjacent islands and true islands implies that tidal marshes restored by moving dikes inland should be able to support tidal channel systems comparable to those of reference marshes not bordered by dikes. Thus allometric relationships generated from reference marshes can provide some standards against which to measure the success of tidal channel restoration in areas necessarily bordered by set-back dikes. Allometric relationships can also provide guidance in planning habitat restoration. For example, scaling exponents for total channel length and total channel surface area are significantly greater than 1 in the Skagit marshes, which means these channel characteristics increase disproportionately with increasing marsh area. If maximizing total channel length and area are restoration goals, one should restore a single large area rather than several smaller areas, i.e., a 100-ha restoration would produce more tidal channel length and surface area than ten separate 10-ha restorations. Another common planning issue is what minimum restorable area is required to support a tidal channel network that meets certain regulatory or biological criteria, and does a particular site meet the threshold. Inverse predictions based on minimum channel count and island magnitude provide limited guidance due to their wide confidence intervals. Likewise the wide range of island areas supporting a single, unbranched tidal channel creates significant uncertainty that derives from the uncertainty of whether tidal channels in the smallest islands will persist or soon fill with sediments. Addressing this issue will require relating channel metrics (e.g., outlet depth or width) to ecological metrics or functions (e.g., fish occupancy, detrital transport, benthic invertebrate density [see *Hood*, 2002a]), or possible surrogates (e.g., inundation period, minimum inundation depth). This information would provide criteria for determining minimum ecologically significant channel widths or depths, where the definition of ecological significance depends on management goals. The minimum ecologically significant channel width or depth would likely not be at the lower limit of the geomorphic data range, so confidence intervals around the inverse estimate of minimum marsh area would be narrowed.

[34] The only other study to scale tidal channel metrics with marsh island area [*Novakowski et al.*, 2004] found scaling exponents of 1.01 and 0.65 for total channel length and trunk length ("maximum mainstream length"), respectively, in a lagoonal estuary in South Carolina (North Inlet Estuary). This value for trunk length scaling agrees with the RIC model and is close to the lower confidence limit for the scaling exponent observed in the Skagit marshes. On the other hand, total channel length scaling differed from that observed in the Skagit or predicted by the RIC model. Further comparisons between different types of tidal marshes would be useful to determine how variable scaling exponents might be, and to learn how differences between sites (e.g., tide range, elevation, substrate character, vegetation type, etc.) affect both scaling exponents and regression elevations. From a practical restoration perspective, it is important to understand what controls site-to-site varia-

tion in scaling patterns to provide generalizable rather than site-specific restoration guidelines. Generating site-specific scaling relationships is problematic for areas where reference marshes no longer exist due to extensive anthropogenic impacts. However, given our current incomplete understanding of tidal channel scaling, extrapolating scaling patterns from one system to another should be done with caution, if at all, as the differences between the North and South Fork marshes show [see also *Hood*, 2002b].

6. Conclusions

[35] 1. Allometric analysis of tidal channel geometry relative to marsh island area produced a variety of scaling relationships that provided a different and complementary perspective on tidal channel geometry compared to traditional approaches based on hydraulic geometry. Metrics describing the set of all channels draining an island (e.g., channel count, maximum channel surface area, length and magnitude, and possibly, median channel surface area, length or magnitude) cannot be analyzed through traditional hydraulic geometry, but can through island allometry. This approach also avoids the potential complication of estimating tidal drainage divides.

[36] 2. Slopes of allometric relationships were uniform among the North Fork, South Fork, and bay fringe marshes, but regression elevations where heterogeneous. The bay fringe marshes had tidal channels several-fold smaller and less complex than those of the North and South Fork marshes. This difference coincides with anthropogenic isolation of river distributaries from the bay fringe marsh and consequent sediment starvation in this area. There were less pronounced, but still significant, differences between the North and South Fork marshes. These may be related to differences in river discharge, distributary abundance relative to total marsh area, exposure to storm fetch, and marsh elevation, among others.

[37] 3. There were no allometric differences between dike-adjacent and true island marsh. This indicates scaling relationships developed in reference marshes can be applied to nearby habitat restoration sites, which are usually adjacent to dikes.

[38] 4. Total channel length and total channel surface area increased disproportionately with marsh island area. This suggests restoring a single large marsh area rather than several smaller areas would maximize potential channel habitat for threatened juvenile Chinook salmon and other estuarine organisms in the Skagit Delta.

[39] 5. Accurate estimation of minimum island area for tidal channel habitat restoration is problematic and will depend on linking ecological criteria to channel metrics.

[40] 6. The RIC model replicates observed scaling patterns of blind tidal channel network structure in the Skagit marshes, thereby linking observed channel network geometry to the previously documented [*Hood*, 2006] process of channel formation through island conglomeration. However, this simplistic model ignores hydrodynamics and sediment transport, and so, cannot address channel width and surface area scaling.

[41] 7. Tidal prism partitioning between channelized and overmarsh flow is likely scale-dependent in the Skagit marshes, and may be so in other tidal marsh systems as well.

References

Allen, J. R. L. (2000), Morphodynamics of Holocene salt marshes: A review sketch from the Atlantic and southern North Sea coasts of Europe, *Quat. Sci. Rev.*, *19*, 1155–1231, doi:10.1016/SO277-3791(99)00034-7.

Beechie, T. J., B. D. Collins, and G. R. Pess (2001), Holocene and recent geomorphic processes, land use, and salmonid habitat in two North Puget Sound river basins, in *Geomorphic Processes and Riverine Habitat*, *Water Sci. Appl.*, vol. 4, edited by J. M. Dorava et al., pp. 37–54, AGU, Washington, D. C.

Boon, J. D. (1975), Tidal discharge asymmetry in a saltmarsh drainage system, *Limnol. Oceanogr.*, *20*, 71–80.

Bull, W. B. (1975), Allometric change of landforms, *Geol. Soc. Am. Bull.*, *86*, 1489–1498.

Church, M., and D. M. Mark (1980), On size and scale in geomorphology, *Prog. Phys. Geogr.*, *4*, 342–390.

Coats, R. N., P. B. Williams, C. K. Cuffe, J. B. Zedler, D. Reed, S. M. Waltry, and J. S. Noller (1995), Design guidelines for tidal channels in coastal wetlands, *Rep. 934*, U. S. Army Corps of Eng., Waterw. Exp. Stn., Vicksburg, Miss.

Collins, B. D., and D. R. Montgomery (2001), Importance of archival and process studies to characterizing pre-settlement riverine geomorphic processes and habitat in the Puget Lowland, in *Geomorphic Processes and Riverine Habitat*, *Water Sci. Appl.*, vol. 4, edited by J. M. Dorava et al., pp. 227–243, AGU, Washington, D. C.

Cowardin, L. M., V. Carter, F. C. Golet, and E. T. LaRoe (1979), *Classification of Wetlands and Deepwater Habitats of the United States*, 79 pp., Fish and Wildlife Serv., U. S. Dep. of Inter., Washington, D. C.

Davidson-Arnott, R. G. D., D. van Proosdij, J. Ollerhead, and L. Schostak (2002), Hydrodynamics and sedimentation in salt marshes: Examples from a macrotidal marsh, Bay of Fundy, *Geomorphology*, *48*, 209–231.

Dragovich, J. D., M. L. Trost, D. K. Norman, G. Anderson, J. Cass, L. A. Gilbertson, and D. T. McKay, Jr. (2000), Geologic map of the Anacortes South and La Conner 7.5-minute quadrangles, Skagit and Island counties, Washington, Wash. State Dep. of Nat. Resour., Olympia.

Fagherazzi, S., A. Bortoluzzi, W. E. Dietrich, A. Adami, S. Lanzoni, M. Marani, and A. Rinaldo (1999), Tidal networks: 1. Automatic network extraction and preliminary scaling features from digital terrain maps, *Water Resour. Res.*, *35*, 3891–3904.

Feola, A., E. Belluco, A. D'Alpaos, S. Lanzoni, M. Marani, and A. Rinaldo (2005), A geomorphic study of lagoonal landforms, *Water Resour. Res.*, *41*, W06019, doi:10.1029/2004WR003811.

Fish and Wildlife Service (1999), Endangered and threatened wildlife and plants: Listing of nine evolutionarily significant units of Chinook salmon, chum salmon, sockeye salmon, and steelhead, *U. S. Fed. Regist.*, *64*, 41,835–41,839.

French, J. R., and T. Spencer (1993), Dynamics of sedimentation in a tide-dominated backbarrier salt marsh, Norfolk, UK, *Mar. Geol.*, *110*, 315–331.

French, J. R., and D. R. Stoddart (1992), Hydrodynamics of salt marsh creek systems: Implications for marsh morphological development and material exchange, *Earth Surf. Processes Landforms*, *17*, 235–252.

Halpin, P. M. (1997), Habitat use patterns of the mummichog, Fundulus heteroclitus, in New England. I. Intramarsh variation, *Estuaries*, *20*, 618–625.

Hood, W. G. (2002a), Landscape allometry: From tidal channel hydraulic geometry to benthic ecology, *Can. J. Fish. Aquat. Sci.*, *59*, 1418–1427.

Hood, W. G. (2002b), Application of landscape allometry to restoration of tidal channels, *Restoration Ecol.*, *10*, 213–222.

Hood, W. G. (2004), Indirect environmental effects of dikes on estuarine tidal channels: Thinking outside of the dike for habitat restoration and monitoring, *Estuaries*, *27*, 273–282.

Hood, W. G. (2006), A conceptual model of depositional, rather than erosional, tidal channel development in the rapidly prograding Skagit River Delta (Washington, USA), *Earth Surf. Processes Landforms*, *31*, 1824–1838.

Hume, T. M. (1991), Empirical stability relationships for estuarine waterways and equations for stable channel design, *J. Coastal Res.*, *7*, 1097–1111.

Leonard, L. A., and M. E. Luther (1995), Flow hydrodynamics in tidal marsh canopies, *Limnol. Oceanogr.*, *40*, 1474–1484.

Levy, D. A., and T. G. Northcote (1982), Juvenile salmon residency in a marsh area of the Fraser River estuary, *Can. J. Fish. Aquat. Sci.*, *39*, 270–276.

Mandelbrot, B. (1983), *The Fractal Geometry of Nature*, W. H. Freeman, New York.

Marani, M., E. Belluco, A. D'Alpaos, A. Defina, S. Lanzoni, and A. Rinaldo (2003), On the drainage density of tidal networks, *Water Resour. Res.*, *39*(2), 1040, doi:10.1029/2001WR001051.

Miller, J. L., and L. R. Gardner (1981), Sheet flow in a salt-marsh basin, North Inlet, South Carolina, *Estuaries*, *4*, 234–237.

Milne, B. T. (1991), Lessons from applying fractal models to landscape patterns, in *Quantitative Methods in Landscape Ecology*, edited by M. G. Turner and R. H. Gardner, pp. 199–235, Springer, New York.

Myrick, R. M., and L. B. Leopold (1963), Hydraulic geometry of a small tidal estuary, *U. S. Geol. Surv. Prof. Pap.*, *411-B*.

Novakowski, K. I., R. Torres, L. R. Gardner, and G. Voulgaris (2004), Geomorphic analysis of tidal creek networks, *Water Resour. Res.*, *40*, W05401, doi:10.1029/2003WR002722.

Odum, W. E. (1984), Dual-gradient concept of detritus transport and processing in estuaries, *Bull. Mar. Sci.*, *35*, 510–521.

Ouchi, S., and M. Matsushita (1992), Measurement of self-affinity on surfaces as a trial application of fractal geometry to landform analysis, *Geomorphology*, *5*, 115–130.

Pethick, J. S. (1992), Saltmarsh geomorphology, in *Saltmarshes: Morphodynamics, Conservation, and Engineering Significance*, edited by J. R. L. Allen and K. Pye, pp. 41–62, Cambridge Univ. Press, New York.

Renger, E., and H.-W. Partenscky (1974), Stabilitätsverhalten von Watteinzugsgebieten, *Kueste Arch. Forschung Tech. Nord. Ostsee*, *25*, 73–86.

Rinaldo, A., S. Fagherazzi, S. Lanzoni, and M. Marani (1999), Tidal networks 2: Watershed delineation and comparative network morphology, *Water Resour. Res.*, *35*, 3905–3917.

Rodriguez-Iturbe, I., and A. Rinaldo (1997), *Fractal River Basins: Chance and Self-Organization*, Cambridge Univ. Press, New York.

Rozas, L. P., C. C. McIvor, and W. E. Odum (1988), Intertidal rivulets and creekbanks: Corridors between tidal creeks and marshes, *Mar. Ecol. Prog. Ser.*, *47*, 303–307.

Sanderson, E. W., S. L. Ustin, and T. C. Foin (2000), The influence of tidal channels on the distribution of salt marsh plant species in Petaluma Marsh, CA, USA, *Plant Ecol.*, *146*, 29–41.

Simenstad, C. A. (1983), The ecology of estuarine channels of the Pacific northwest: A community profile, *Rep. FWS/OBS 83/05*, U. S. Fish and Wildlife Serv., Washington, D. C.

Sokal, R. R., and F. J. Rohlf (1995), *Biometry*, W. H. Freeman, New York.

Temmerman, S., T. J. Bouma, G. Govers, and D. Lauwaet (2005), Flow paths of water and sediment in a tidal marsh: Relations with marsh developmental stage and tidal inundation height, *Estuaries*, *28*, 338–352.

Williams, G. D., and J. B. Zedler (1999), Fish assemblage composition in constructed and natural tidal marshes of San Diego Bay: Relative influence of channel morphology and restoration history, *Estuaries*, *72*, 702–716.

Williams, P. B., M. K. Orr, and N. J. Garrity (2002), Hydraulic geometry: A geomorphic design tool for tidal marsh channel evolution in wetland restoration projects, *Restoration Ecol.*, *10*, 577–590.

Woldenberg, M. J. (1966), Horton's laws justified in terms of allometric growth and steady state in open systems, *Geol. Soc. Am. Bull.*, *77*, 431–434.

Zar, J. H. (1984), *Biostatistical Analysis*, Prentice-Hall, Upper Saddle River, N. J.

Zeff, M. L. (1999), Salt marsh tidal channel morphometry: Applications for wetland creation and restoration, *Restoration Ecol.*, *7*, 205–211.

―――――――――――――

W. G. Hood, Skagit River System Cooperative, P.O. Box 368, LaConner, WA 98257, USA. (ghood@skagitcoop.org)